Dearomative Skeletal Editing of Benzenoids via Diradical

Xiang-Xin Zhang,[‡,§,] Shan-Tong Xu,[‡] Xue-Ting Li,[‡,§] Ting-Ting Song,[‡] Ding-Wei Ji,[‡] Qing-An Chen[*,‡,§]

[‡]Dalian Institute of Chemical Physics, Chinese Academy of Sciences, Dalian 116023, People's Republic of China

[§]University of Chinese Academy of Sciences, Beijing 100049, People's Republic of China

*Corresponding author: E-mail: qachen@dicp.ac.cn, Web: www.lbcs.dicp.ac.cn

ABSTRACT:

Dearomative skeletal editing of benzenoids represents a promising yet challenging strategy for the rapid construction of high-value carbon frameworks from readily accessible starting materials. Büchner reaction is a unique type of dearomatizative ring expansion that transforms benzenoids into functionalized cycloheptatrienes (CHTs). However, due to challenges in compatibility and selectivity, achieving seamless integration of this reaction with upgrading transformations within a unified system remains undeveloped. Here, we demonstrated an energy transfer–induced intermolecular dearomative skeletal editing reaction of benzenoids with a range of electronically diverse alkynes. This protocol employed *N*-acylimines as diradical precursors to efficiently construct various formally rearranged heteropropellanes in high chemo-, regio- and diastereoselectivities that have been previously inaccessible. The challenges related to general reactivity and selectivity issues were circumvented through smooth merging of the photoinduced Büchner reaction with radical [6+2] cycloaddition. Experimental and computational studies have been performed to support diradical mechanism and interpret the origins of the observed chemo-, regio- and diastereoselectivities.

INTRODUCTION

As bulk and fundamental chemical feedstocks, benzenoids play important roles in chemistry, materials, medicines, etc. Due to its inherent aromaticity[1], the delocalization of the π-electrons makes it particularly stable, so that many approaches to benzenoid transformations are concentrated in the functionalization of peripheral C-H or C-X bonds (Fig. 1a)[2-7]. Recently, the "escape from flatland" concept[8,9], which transforms planar aromatic rings into three-dimensional (3D) scaffolds, has become a key strategy in modern drug discovery for optimizing molecular properties and enhancing target interactions. Notably, the dearomatization has become an increasing cornerstone of the synthetic methodology, serving as a critical tactic for disrupting molecular planarity[10-14]. Especially for benzenoids, a variety of strategies have been developed to achieve their dearomatization, such as dearomative hydrogenation[15], Birch reduction[16], dearomatization of phenols[17], transition metal[18] or arenophile[19]-mediated dearomatizations. These transformations could convert simple benzene derivatives into high-value and synthetically versatile compounds. However, they still retain the inherent framework of the arenes. The dearomative skeletal editing (DASE) of the carbon skeleton of benzenoids, while simultaneously increasing the complexity of the framework, is still in its infancy[20-22]. Meanwhile, given the significant applications of propellanes in material science, drug discovery, and natural product

synthesis[23], the construction of formally rearranged heteropropellanes directly from aromatic rings is of great interest in synthetic chemistry.

As a unique type of expansive dearomatization, Büchner reaction has become a practical and effective strategy for directly constructing valuable functionalized CHTs from simple aromatic precursors[24]. Generally, the Büchner reaction refers to the cyclopropanation of a double bond of benzenoid with carbene to generate a norcaradiene (NCD) intermediate. Subsequently, it is transformed into a more stable CHT through electrocyclic rearrangement (Fig. 1b). Since the reaction was firstly reported by Büchner and Curtius in 1885[25], significant advancements have been achieved in Büchner reaction through the rational design of substrates and catalysts to enhance the reactivity and selectivity (Fig. 1c)[24,26-36]. For example, the Jiang group[34] achieved a photoinduced version of the Büchner reaction by employing light-induced carbene generation. Similarly,

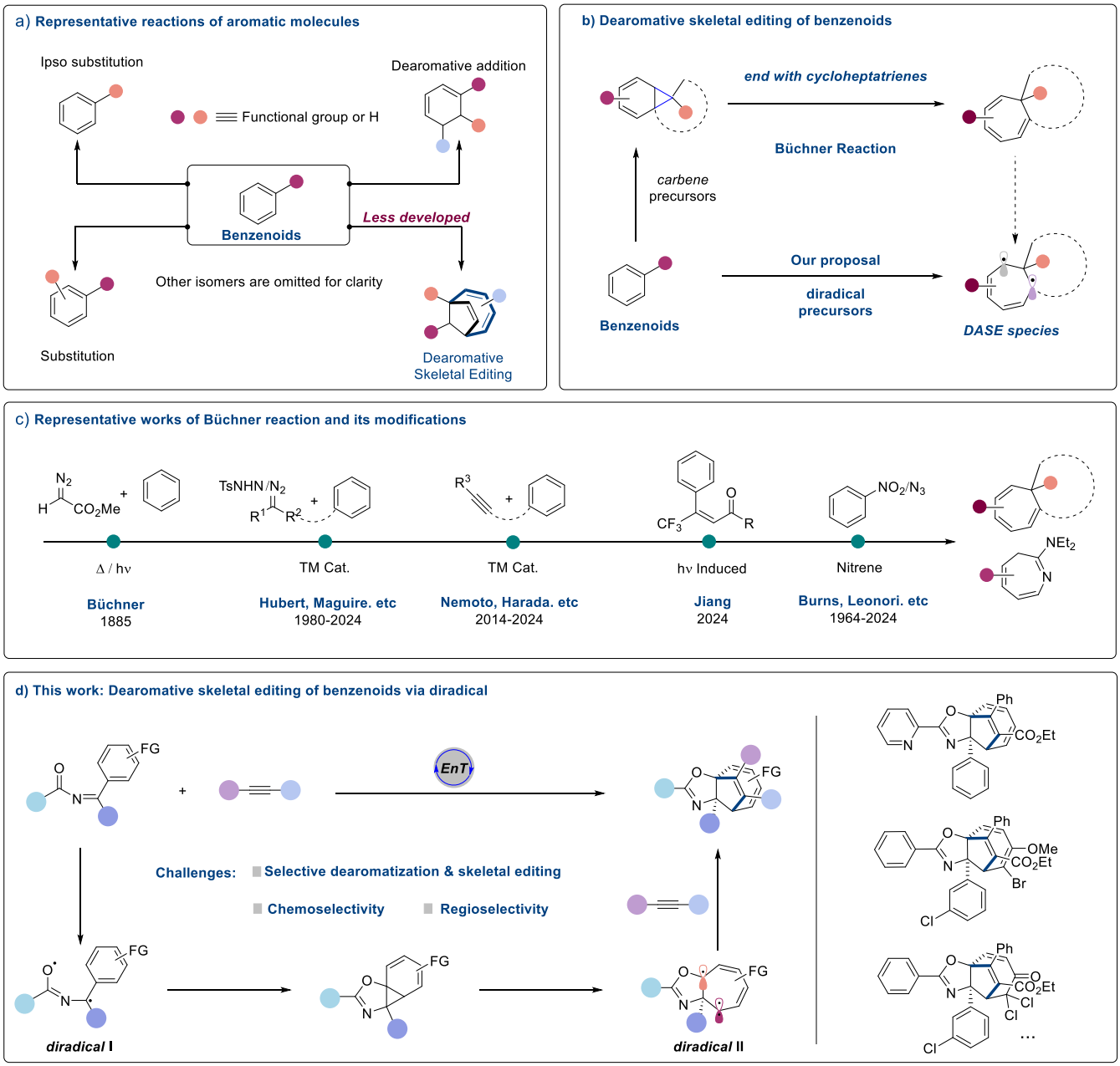

Fig. 1. Approaches to polycyclic structures through dearomative skeletal editing of benzenoids.

the aza-variants of the Büchner reaction could be accomplished through the generation of nitrenes, resulting in the formation of the corresponding azepines[28,29,37]. Although these elegant works have extended the breadth of the Büchner reaction, most efforts have remained focusing on generating the corresponding CHTs and azepines. Accordingly, only a few reports have tried to explore further transformations of the Büchner reaction via sophisticated design of the substrates (2D to 3D)[32,33,38]. Developing a concise and efficient protocol to integrate new transformations with the Büchner reaction will significantly broaden the chemical space, thereby increasing structural diversity and expanding its applications.

Energy transfer catalysis (EnT)[39-41] has been rapidly developed, enabling traditionally unreactive substrates to be efficiently transformed through radical intermediates under mild conditions. Considering the current situation, we wonder if the generated CHT intermediate of Büchner reaction could be transformed into a diradical via energy transfer, enabling its participation in subsequent reactions and thus overcoming previous reaction limitations. Meanwhile, it remains to be determined whether a new and atom-economic precursor could be developed to react with benzenoids, replacing traditionally used carbene precursors.

N-Acylimines are frequently used as precursors in the synthesis of substituted amines[42], amino alcohols[43], and amino acids[44,45]. The majority of these reactions proceed via radical anion intermediates. However, the application of this substance as a precursor in the Büchner reaction or its involvement as a diradical precursor has not yet been demonstrated. Additionally, the presence of various diradicals (Fig. S2) could cause counterproductive side reactions with radical receptors (Fig. S3). Moreover, the equilibrium between the NCD and CHT[46] presents another issues in chemo-, regio- and diastereoselectivities that still need to be addressed. Inspired by the precedent progress on Büchner reaction, we herein developed a protocol of photochemical dearomative skeletal editing of benzenoids with alkynes under energy transfer catalysis (Fig. 1d). It demonstrated that *N*-acylimines could be used as new and atom-economic diradical precursors to facilitate an upgraded Büchner reaction, seamlessly generating CHT diradicals to create complex three-dimensional polycyclic skeletons.

RESULTS AND DISCUSSION

Reaction optimization. We began our investigation with the use of *N*-(diphenylmethylene) benzamide (**1a**) and ethyl 3-phenylpropiolate (**2a**) as reaction partners (Table 1). After careful optimization, tricyclo [4.4.2.0^{1,5}] product **3** was obtained in 76% isolated yield under standard conditions with **PC-1** (2-chloro-9H-thioxanthen-9-one) as a photocatalyst with good chemo- and regioselectivity (entry 1). The effect of other reaction parameters on this aromatic dearomative skeletal editing was further evaluated. Varying the wavelength of reaction greatly decreased the yields (entry 2). Moreover, through the investigation of photocatalysts, only Ir[dF(CF$_3$)ppy]$_2$[dtbbpy]PF$_6$, Ir(dF-ppy)$_3$, **PC-1** and its derived photocatalysts could promote the desired dearomative skeletal editing (entries 3-5 and Table S1 in Supplementary Information). Additionally, other solvents, such as ethyl acetate (EA), dichloromethane (DCM), methanol (MeOH) and dimethylsulfoxide (DMSO) led to a substantial decrease in reaction yields (entries 6-10). Changing different additives and the concentration of the reaction had slightly unfavorable ef-

fects on the yields (entry 11 and Tables S5 and S6 in Supplementary Information). The presence of photocatalyst and light irradiation were essential in this reaction (entries 12 and 13).

Table 1. Optimization for dearomative skeletal editing of benzenoids

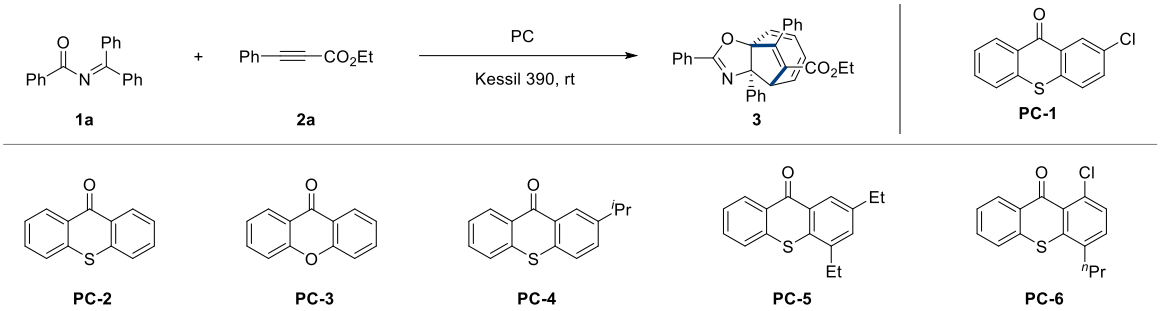

Entry	Deviation from standard conditions	**3** (%)[a]
1	None	95 (76[b])
2	427 nm, 456 nm, Blue LED	11, 4, --
3	$[Ru(bpy)_3](BF_4)_2$, *fac*-$[Ir(ppy)_3]$, $[Mes\text{-}Acr](ClO_4)$	--
4	$[Ir(dF(CF_3)ppy)_2(dtbbpy)]PF_6$	21
5	**PC-2**, **3, 4, 5, 6**	56, --, 63, 68, 18
6	EA	34
7	DCM	28
8	DMF	35
9	MeOH	11
10	DMSO	44
11[c]	$Zn(OAc)_2$	57
12	w/o PC	--
13	dark, 70 ºC	--

Conditions: **1a** (0.20 mmol), **2a** (0.50 mmol), **PC-1** (0.04 mmol), $ZnCl_2$ (0.20 mmol), MeCN (0.5 mL), Kessil 390 nm, 40 W, rt, 24 h; [a]Determined by HPLC with anthracene as internal standard; [b]Isolated yield; [c]**1a** (0.20 mmol), **2a** (0.22 mmol), **PC-1** (0.02 mmol), $Zn(OAc)_2$ (0.20 mmol), MeCN (2.0 mL).

Substrate scope. With the optimal conditions in hand, we systematically explored the substrate scope of this dearomative skeletal editing approach (Fig. 2). A wide range of *N*-acylimines all underwent smoothly, delivering corresponding formally rearranged heteropropellanes with excellent chemo- and regio-selectivities. For aromatic ring (R = Ar^1) conjugated with the carbonyl group, a series of functional groups, including OMe (**4**, **7**, **9**), bromo (**5**), ester (**6**) and chloro (**8**, **10**, **11**), were well accommodated irrespective of their substituent positions, providing good opportunities for further transformations. Meanwhile, the robustness of this protocol was demonstrated by its compatibility with other (hetero)aromatic groups (**12**-**14**). Naphthyl (**12**) and thienyl (**13**) groups, which are typically influenced by energy transfer catalysis, remained unaffected under the conditions of this protocol. Notably, pyridyl group also exhibited good compatibility (**14**), enabling the construction of a potentially novel pyridine−oxazoline type ligand in one step. The structural variety of the ligand could be further enriched by changing the substituents of pyridines and subsequent modifications of the products. The alkyl group could also be applicable to this reaction when stronger UV light irradiation was used (**15**), which further expanded the scope of this reaction.

Next, a series of aromatic ring (Ar^2) associated with the imine moiety were investigated under the standard conditions (Fig. 2). Gratifying, modifying the position of aromatic ring substituents enabled the selective introduction of different substituents into distinct positions of conjugated dienes within seven-membered rings (**16**-**22**). For example, adjustment of the methyl group position on the aromatic ring (ortho, meta and para) enabled predictable incorporation into specific positions of the seven-membered ring moiety (**16**, **20**, **20'** and **22**). Similarly, methoxy-substituted conjugated diene units were efficiently assembled (**17**), enabling the rapid construction of multi-functionalized tropilene derivatives. Notably, halogenated conjugated diene structural units, which are challenging to construct, could also be accessed using this protocol (**18**, **19**, **21** and **21'**). The presence of OMe group on Ar^2 could generally give better performance. Moderate to high yields could be obtained for *N*-acylimines bearing electron-donating and -withdrawing substituents on the aromatic ring Ar^1 (**23**-**31**). This further expanded the structural diversity and functional group variety, facilitating subsequent construction of diverse polycyclic structures. Furthermore, for unsymmetric imines, selectively dearomative skeletal editing of one of the aromatic ring Ar^2 was implemented smoothly (**32**-**37**). Substrates bearing a single substituent, either *para*-methoxy (**32**), *meta*-chloro (**34**), or *ortho*-methyl (**35**), selectively yielded their respective products in high regioselectivities. For *para*-chloro substrate, the reaction predominantly proceeding via dearomative skeletal editing of non-substituted aromatic ring (**33**). Notably, two different substituents could be introduced simultaneously into conjugated diene structures (**36**). For different aromatic rings containing substituents with varying properties, selective destruction of the aromaticity of one of the aromatic rings could also be achieved efficiently (**37**). When enones (**1aj** and **1ak**[34]) were used instead of *N*-acylimines, no corresponding products were detected (**38** and **39**). It indicates that the introduction of the nitrogen atom in the substrate is crucial for this protocol. The assignment of chemo-, regio- and stereoselectivities of this protocol was determined by crystal analysis of representative products **18**, **35**-**37**.

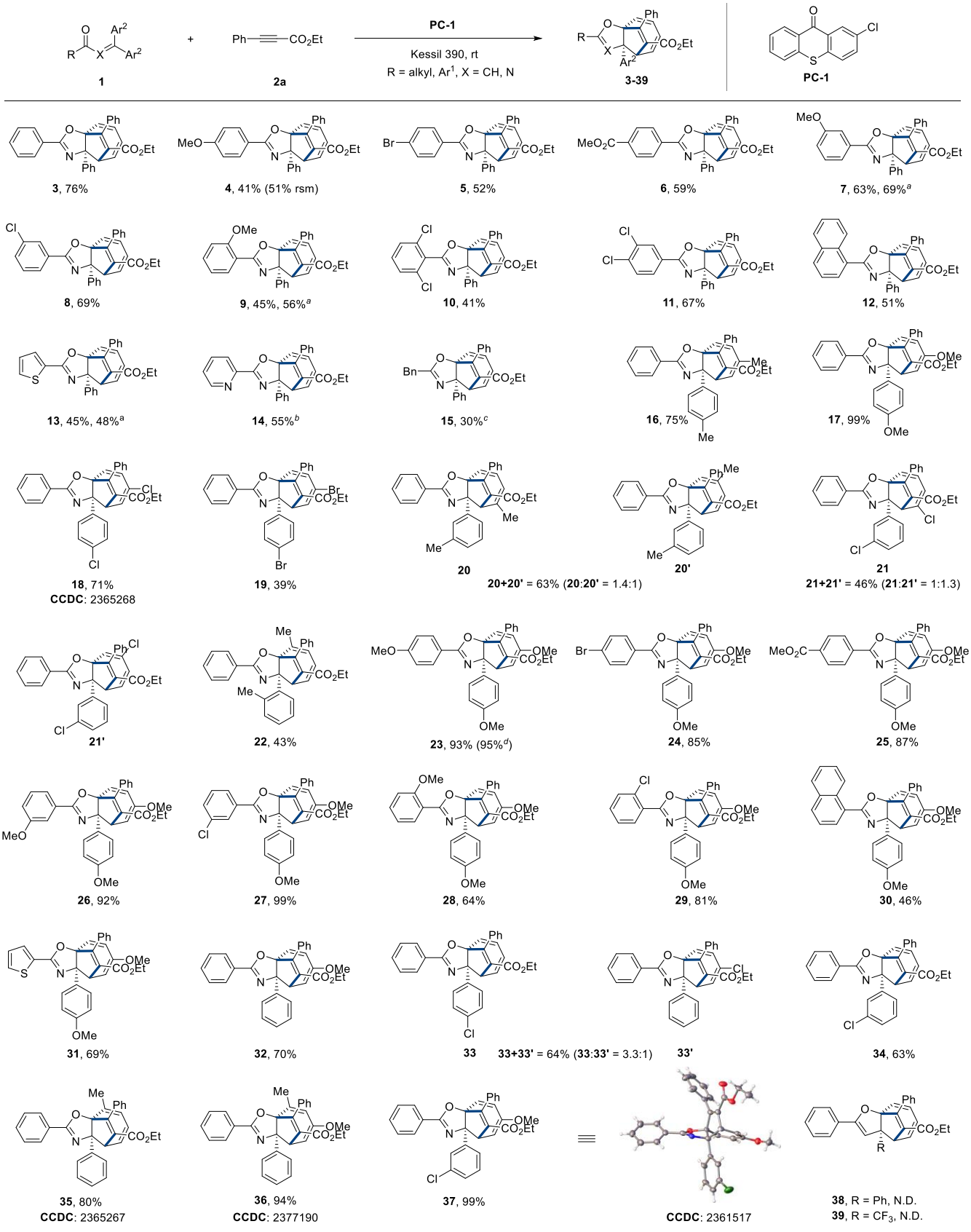

Fig. 2. Substrate scope of *N*-acylimines. Conditions: **1** (0.20 mmol), **2a** (0.50 mmol), **PC-1** (0.04 mmol), $ZnCl_2$ (0.20 mmol), MeCN (0.5 mL), Kessil 390 nm, 40 W, rt, 24 h. Isolated yields were given; [a]48 h; [b]No $ZnCl_2$, MeCN:DCM = 1:1 (0.5 mL); [c]365 nm, 50 W; [d]No $ZnCl_2$.

To expand the application range of substrates, subsequently, a series of alkynes were evaluated (Fig. 3). Fortunately, a wide range of different substituted phenylpropiolates could be well tolerated in this protocol, irrespective of their electronic factors (**40**-**48**). The positional variation of the substituents had a minimal effect on the reaction (**41** vs **46**, **44** vs **45**). By slightly changing the reaction conditions, the applicability of the reaction was further extended. 4-Phenylbut-3-yn-2-one containing both alkynyl and carbonyl groups that are susceptible to energy transfer catalytic reaction was also compatible with this method (**49** and **50**). Besides, simple phenylacetylene could be well accommodated in this protocol (**51**). The resulting trisubstituted alkene was preserved under the reaction condition without undergoing further side reaction.

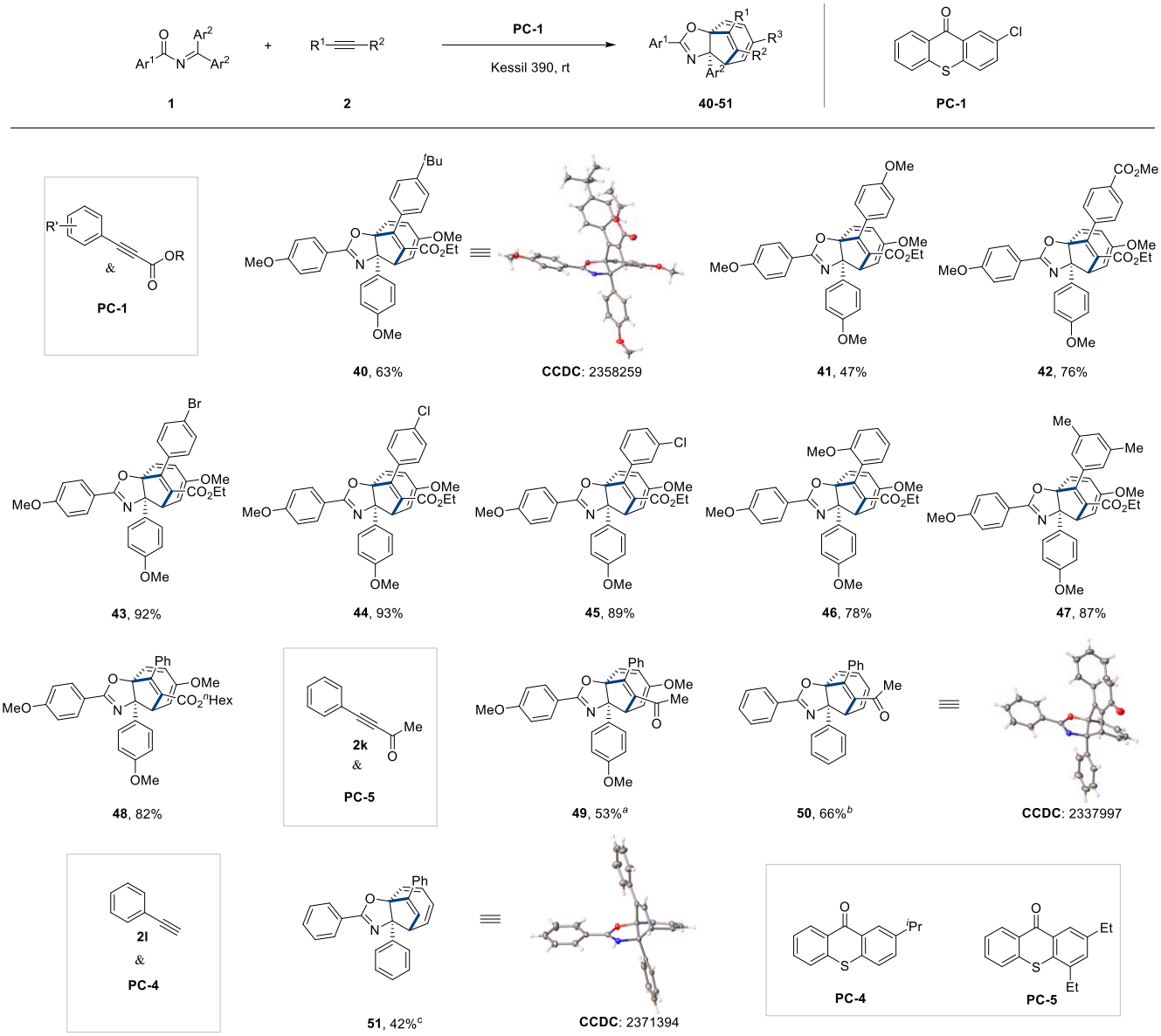

Fig. 3. Substrate scope of alkynes. Conditions: **1t** (0.20 mmol), **2** (0.50 mmol), **PC-1** (0.04 mmol), $ZnCl_2$ (0.20 mmol), MeCN (0.5 mL), Kessil 390 nm, 40 W, rt, 24 h; [a]**2k** (0.60 mmol), **PC-5** (0.03 mmol), MeCN (1.0 mL), Kessil 390 nm, 40 W, rt, 24 h; [b]**1a** (0.20 mmol), **2k** (0.50 mmol), **PC-5** (0.03 mmol), $Mn(OAc)_2$ (0.20 mmol), MeCN (2.0 mL), 390 nm, 100 W, rt, 24 h; [c]**2l** (1.0 mmol), **PC-4** (0.03 mmol), $ZnCl_2$ (0.20 mmol), ^{i}PrOH (1.0 mL), 390 nm, 50 W, rt, 24 h; Isolated yields were given in all cases.

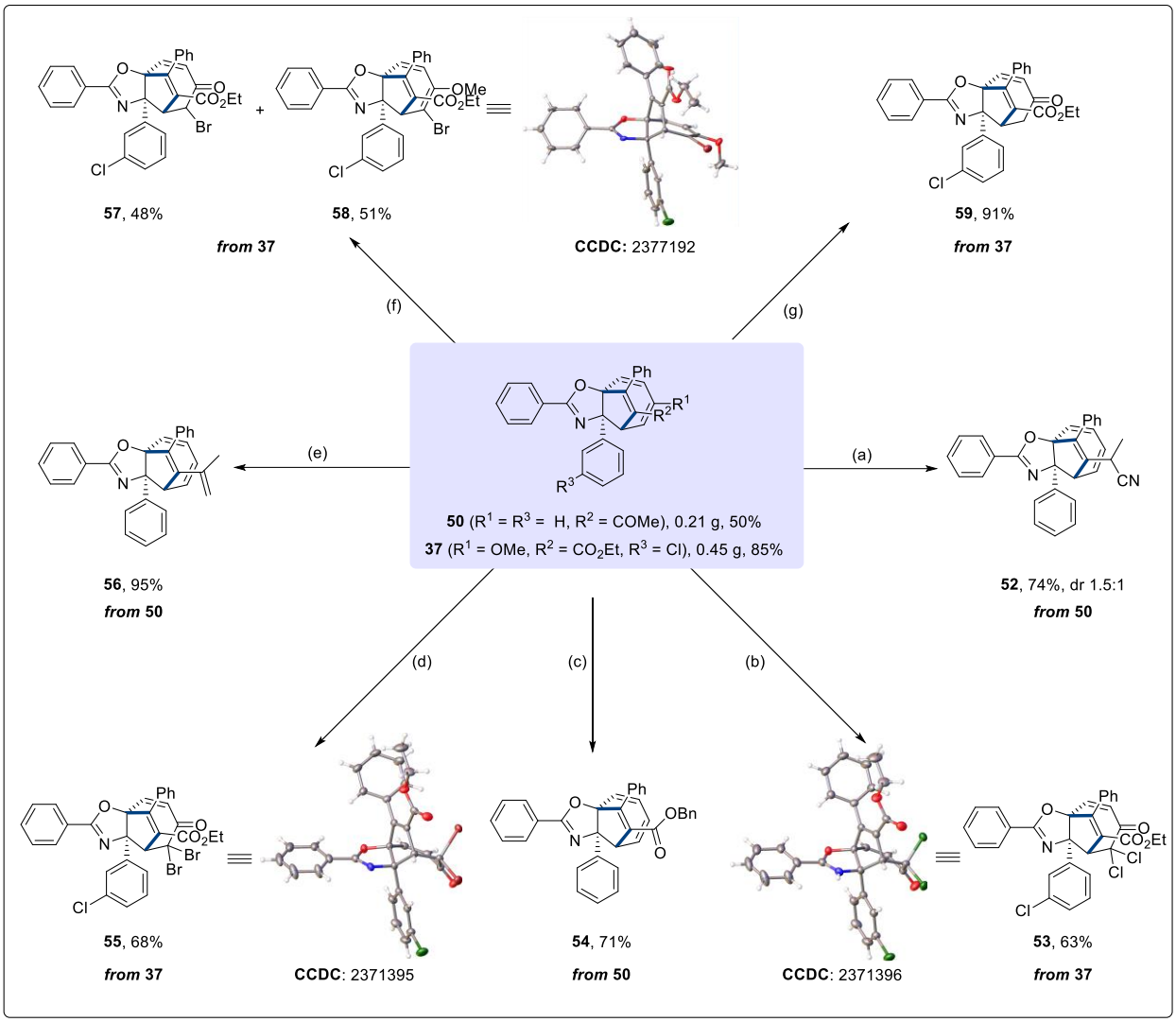

Fig. 4. Synthetic derivatizations for constructing polyfunctional polycyclic structures. Conditions: (a) **50** (0.10 mmol), TosMIC (0.15 mmol), ^{t}BuOK (0.25 mmol), DME (0.6 mL), ^{t}BuOH (0.2 mL), 0 ºC - rt, 6 h; (b) **37** (0.10 mmol), NCS (0.20 mmol), $Sc(OTf)_3$ (0.10 mmol), DCM (1.0 mL), rt, 18 h; (c) **50** (0.10 mmol), I_2 (0.30 mmol), DBU (0.40 mmol), BnOH (0.11 mmol), DCM (1.0 mL), 0 ºC - rt, 16 h; (d) **37** (0.10 mmol), NBS (0.20 mmol), $Sc(OTf)_3$ (0.10 mmol), DCM (1.0 mL), rt, 18 h; (e) **50** (0.10 mmol), $MePPh_3Br$ (0.36 mmol), ^{t}BuOK (0.40 mmol), THF (1.0 mL), 0 ºC - rt, 12 h; (f) **37** (0.10 mmol), $CuBr_2$ (0.20 mmol), DCM (0.5 mL), 70 ºC, 12 h; (g) **37** (0.10 mmol), MeOH (0.13 mmol), TFA (0.5 mL), DCM (1.0 mL), 70 ºC, 8 h.

In order to demonstrate the comprehensive utility of the protocol, various transformations were performed (Fig. 4). Scale-up reactions for representative compounds **37** and **50** were successfully performed following this protocol, demonstrating its effectiveness and reproducibility on a larger scale. For product **50** containing methyl ketone structure, the conversion of the carbonyl to cyano group was achieved through the Van Leusen reaction (**52**). Take advantage of enol isomerization, a polycyclic skeleton containing tropilene structural units could be synthesized with **37** serving as the substrate (**53**, **55**, **57**-**59**). Remarkably, two halogen (Cl or Br) substituents could also be introduced into the alpha position of the carbonyl group at the same time with the addition of electrophiles (**53** and **55**). A conjugated diene unit containing both Br and OMe was constructed by electrophilic substitution (**58**), and *α*-bromo-unsaturated ketone structure could be obtained by isomerization of enol (**57**).

Furthermore, ketone-to-ester transformation was achieved by haloform coupling reaction of **50** with benzyl alcohol (**54**). Polycyclic compound containing polyene skeleton could be accessed via Witting reaction (**56**). The assignment of stereochemistry of products **53**, **55**, and **58** was further confirmed through single crystal X-ray crystallography.

Mechanistic investigations. To gain insight into the mechanistic underpinnings of this dearomative skeletal editing protocol, a series of mechanism experiments were performed (Fig. 5). UV/Vis spectroscopy of the reaction components revealed that **PC-1** was the only light absorbing species around a wavelength of 390 nm (Fig. 5a). This result also excluded the possibility of direct excitation of **1a** or **2a**, as well as the formation of a photoexcited EDA complex between **1a** and **2a**. In addition, Stern-Volmer quenching studies clearly demonstrated that **1a** quenched the excited photocatalyst (**PC-1***), while **2a** had no detectable quenching (Fig. 5b). Light on/off experiments indicated that the irradiation of visible light was indispensable (Fig. 5c). The corresponding Büchner reaction product **60** could be isolated in the absence of alkyne **2a** (Fig. 5d). The side product **61** was probably formed through the diradical A. The direct excitation experiment with stronger UV light (λ_{max} = 365 nm) of the standard reaction gave 4% yield after 96 h (Fig. 5e). When the phenyl group was replaced by benzyl group, no corresponding product was detected (Table S13), indicating that the reaction was probably initiated by the sensitization of the carbonyl group (via diradical B). When the intermediate **60** was employed in the reaction, it was found that the corresponding desired product **23** could be obtained only under standard condition. It could not be obtained in the absence of photocatalyst or only heating. On the contrary, the associated substrate **1t** was recovered under thermal condition (Fig. 5f).

Next, a series of photocatalysts with different triplet energies were tested (Fig. 5g). The yields exhibited a general trend of increasing with the rise in triplet energy, while no relation was found on the redox potentials. The kinetic experiments showed that Büchner product **60** was predominantly generated in the first half hour, then gradually decreased with time. Meanwhile, the corresponding product **23** progressively increased over time (Fig. 5h). Subsequently, a series of radical inhibition experiments were carried out (Fig. 5i). The reaction was significantly or completely inhibited by adding a variety of free radical inhibitors (2,2,6,6-tetramethylpiperidinoxy, TEMPO; 5,5-dimethyl-1-pyrroline *N*-oxide, DMPO; butylated hydroxytoluene and BHT) to the reaction mixture. These results suggested a radical pathway was probably involved in this reaction. Meanwhile, in the presence of triplet quencher (O_2 or 2,5-dimethylhexa-2,4 diene), the reaction was also greatly or completely inhibited, suggesting that the reaction was most likely mediated via energy transfer catalysis. Notably, in the presence of DMPO, a new compound with $[M+H]^+$ of 489.2359 was detected (Fig. S10). Therefore, radical trapping experiments were carried out (Fig. 5j). When DMPO was used as the spin trapping reagent[47], two interesting products (**62** and **63**) of the reaction of **1t** with DMPO could be isolated and verified by X-ray crystallography. It indicated that the reaction probably took place via diradical intermediate.

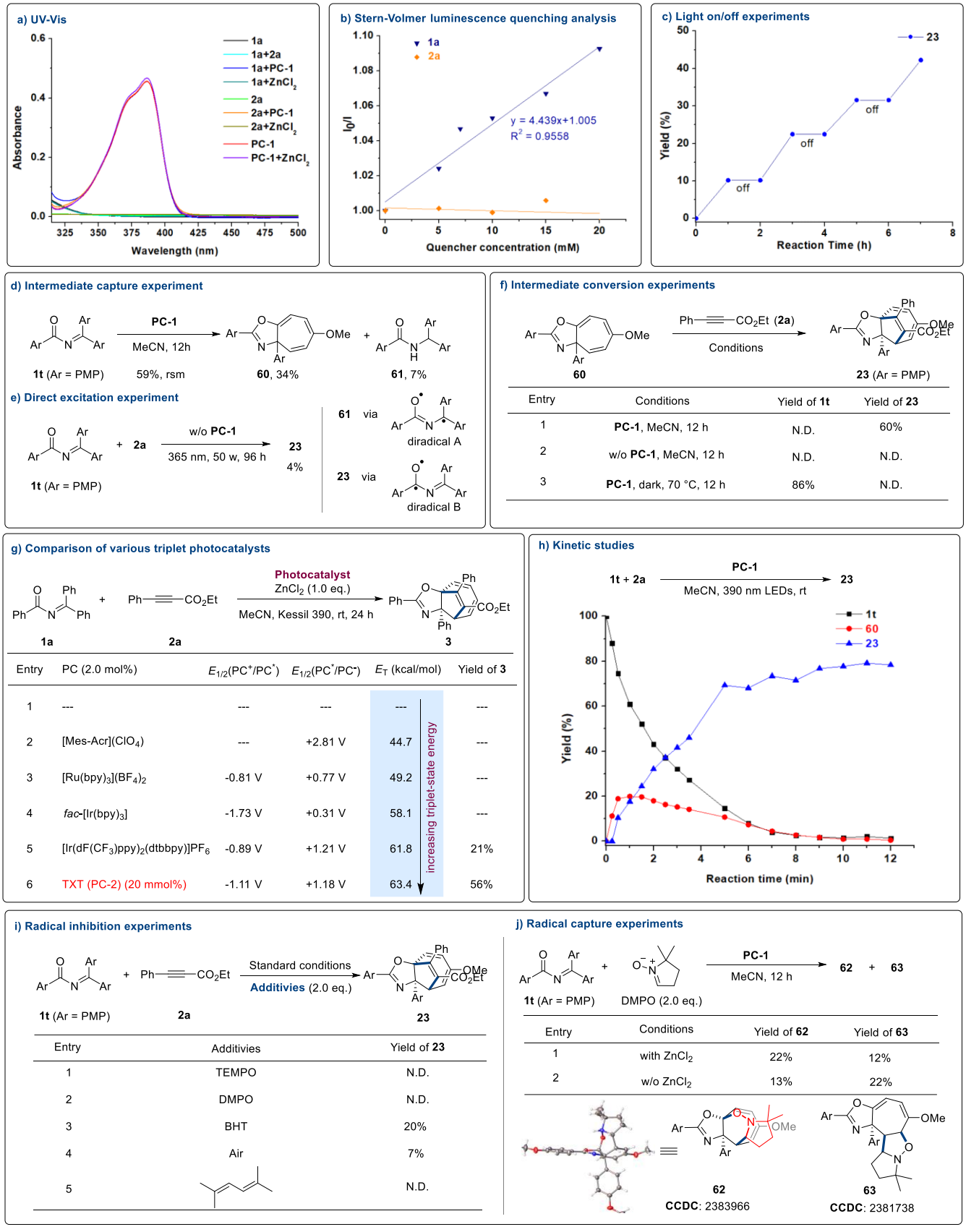

Entry	PC (2.0 mol%)	$E_{1/2}(PC^+/PC^*)$	$E_{1/2}(PC^*/PC^-)$	E_T (kcal/mol)	Yield of **3**
1	---	---	---	---	---
2	$[Mes\text{-}Acr](ClO_4)$	---	+2.81 V	44.7	---
3	$[Ru(bpy)_3](BF_4)_2$	-0.81 V	+0.77 V	49.2	---
4	*fac*-$[Ir(bpy)_3]$	-1.73 V	+0.31 V	58.1	---
5	$[Ir(dF(CF_3)ppy)_2(dtbbpy)]PF_6$	-0.89 V	+1.21 V	61.8	21%
6	TXT (PC-2) (20 mmol%)	-1.11 V	+1.18 V	63.4	56%

increasing triplet-state energy

Entry	Conditions	Yield of **1t**	Yield of **23**
1	**PC-1**, MeCN, 12 h	N.D.	60%
2	w/o **PC-1**, MeCN, 12 h	N.D.	N.D.
3	**PC-1**, dark, 70 °C, 12 h	86%	N.D.

Entry	Additivies	Yield of **23**
1	TEMPO	N.D.
2	DMPO	N.D.
3	BHT	20%
4	Air	7%
5		N.D.

Entry	Conditions	Yield of **62**	Yield of **63**
1	with $ZnCl_2$	22%	12%
2	w/o $ZnCl_2$	13%	22%

Fig. 5. Mechanism experiments

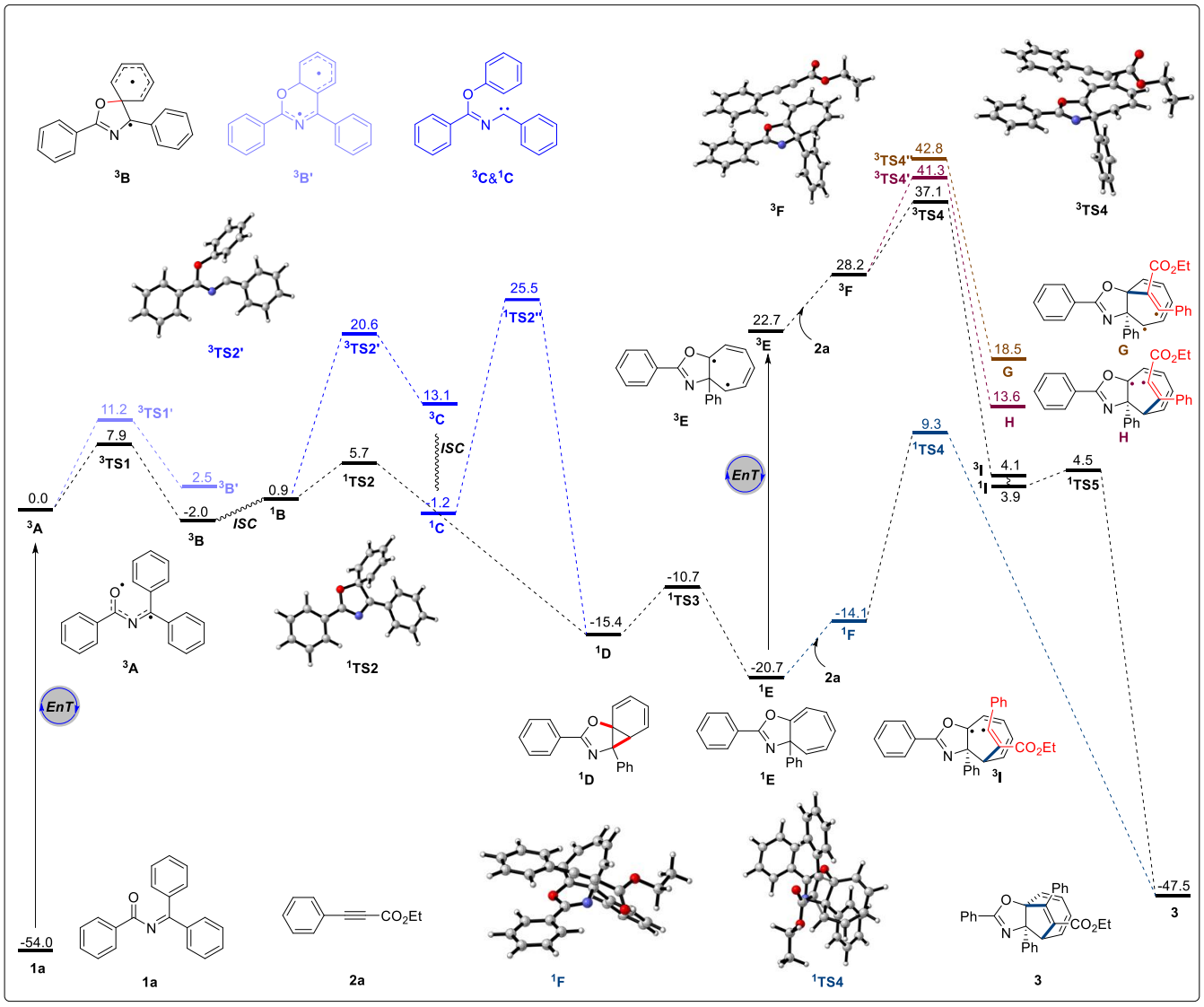

Fig. 6. Reaction mechanism

Based on the aforementioned mechanistic studies and further DFT calculations, a plausible energy transfer mechanism is shown in Fig. 6. Visible light excited PC sensitizes *N*-(diphenylmethylene) benzamide (**1a**) by EnT, which subsequently produces the diradical ^{3}**A**. Then the oxygen radical of ^{3}**A** attacks the benzene ring to produce the corresponding dearomatic diradical intermediate ^{3}**B** via ^{3}**TS1**. The intersystem crossing of the generated triplet 1,3-diradical allows subsequent radical-radical recombination to produce the corresponding NCD intermediate ^{1}**D** via ^{1}**TS2** ($\Delta G_2^{\ddagger}$ = 4.8 kcal/mol). Moreover, the formation of ^{1}**D** via the generation of the corresponding carbene ^{3}**C** followed by the Büchner reaction is excluded (^{3}**TS2'**, $\Delta G_2^{\ddagger}$ = 19.7 kcal/mol). Afterwards, the norcaradiene ^{1}**D** undergoes electrocyclization rearrangement to generate CHT intermediate ^{1}**E**. Subsequently, the excited PC sensitizes ^{1}**E** by EnT and the resulting triplet state ^{3}**E** approaches ethyl 3-phenylpropiolate (**2a**) to form an exciplex ^{3}**F**. This exciplex results in the formation of first C–C bond between ^{3}**E** and alkyne **2a**, which determines the regioselectivity. Furthermore, the process of directly obtaining ^{3}**E** from sensitized ^{1}**D** is not feasible (via ^{3}**TS3**, $\Delta G_3^{\ddagger}$ = 14.7 kcal/mol, Fig S11). DFT calculations disclose that the transition state in which the pure carbon radical of ^{3}**E** engages **2a** in the 2-position is thermodynamically most favorable ($\Delta G_4^{\ddagger}$ = 8.9 kcal/mol), leading to the observed regioisomer. Other regional

isomers are required to overcome higher free energy barriers, 13.1 kcal/mol (via ^{3}**TS4**') and 14.6 kcal/mol (via ^{3}**TS4''**). The resulting intersystem crossing of the triplet 1,5-diradical allows subsequent *cis*-selective radical-radical recombination as a diastereoselective determining step, resulting in final dearomative skeletal editing product **3**. Meanwhile, both theory and experiment excluded the possibility of the [6+2] cycloaddition of ^{1}**E** and **2a** in the ground state to obtain the target product **3** (via ^{1}**TS4**, $\Delta G^{1}{}_{4}{}^{\ddagger}$ = 23.4 kcal/mol).

CONCLUSION

In conclusion, a general strategy for dearomative skeletal editing of benzenoids has been developed by smooth merging of the photoinduced Büchner reaction with radical [6+2] cycloaddition. The generation of critical dearomative cycloheptatriene diradical is contingent upon the strategic design of diradical precursors and the sequential iteration of diverse diradical species. This strategy features excellent chemo-, regio- and diastereoselectivities and broad functional group tolerance. A series of structurally diverse polycyclic frameworks can be obtained simply by modifying the substituents on the aromatic ring. The experimental and computational results indicate that the rapid iteration of multiple diradicals and their matching with alkynes is crucial for achieving highly selective dearomatization and skeletal editing of benzenoids. Synthetic derivatizations further prove the practicability of the strategy.

METHODS

General procedures for the synthesis of desired dearomative skeletal editing products. In a glove box, an oven-dried 4 mL vial was charged with **1** (0.20 mmol), alkyne (0.50 mmol), **PC-1** (0.04 mmol), MeCN (0.5 mL), $ZnCl_2$ (0.20 mmol) at room temperature. The reaction tube was sealed with a Teflon screw cap, removed from the glove box. Then, the reaction mixture was stirred at rt under Kessil 390 nm (40 W) for 24 hours. And the crude reaction mixture was purified by column chromatography on silica gel using petroleum ether and ethyl acetate to afford the corresponding product. Notes: as for alkyne **2k**, **PC-5** (0.03 mmol), MeCN (1.0 or 2.0 mL), $Mn(OAc)_2$ (0.20 mmol); as for alkyne **2l**, **PC-4** (0.03 mmol), $ZnCl_2$ (0.20 mmol), ^{i}PrOH (1.0 mL), 390 nm, 50 W.

ACKNOWLEDGEMENTS

Financial support from the National Natural Science Foundation of China (22071239) is acknowledged.

AUTHOR CONTRIBUTIONS

Q.-A. C. supervised the project. Q.-A. C. and X.-X. Z. conceived and designed the experiments. X.-X. Z., S.-T. X., X.-T. L. performed the synthetic experiments. T.-T. S. analyzed the X-ray structures. Q.-A. C., X.-X. Z. and D.-W. J. analyzed the data. All authors discussed the results and commented on the manuscript.

DATA AVAILABILITY

The X-ray crystallographic data for compounds have been deposited in the Cambridge Crystallographic Data Centre (CCDC). Data relating to the characterization data of materials and products, general methods, optimization studies, experimental procedures, mechanistic studies, mass spectrometry and NMR spectra are available in the Supplementary Information. All data are also available from the corresponding author upon request.

COMPETING INTERESTS

The authors declare no competing interests.

REFERENCE

1 von Schleyer, P. R. & Jiao, H. What is aromaticity? *Pure Appl. Chem.* **68**, 209-218 (1996).

2 Wang, C.-S., Dixneuf, P. H. & Soulé, J.-F. Photoredox Catalysis for Building C–C Bonds from C(sp2)–H Bonds. *Chem. Rev.* **118**, 7532-7585 (2018).

3 Wang, H., Gao, X., Lv, Z., Abdelilah, T. & Lei, A. Recent Advances in Oxidative R1-H/R2-H Cross-Coupling with Hydrogen Evolution via Photo-/Electrochemistry. *Chem. Rev.* **119**, 6769-6787 (2019).

4 Wang, J. & Dong, G. Palladium/Norbornene Cooperative Catalysis. *Chem. Rev.* **119**, 7478-7528 (2019).

5 Shi, J., Li, L. & Li, Y. o-Silylaryl Triflates: A Journey of Kobayashi Aryne Precursors. *Chem. Rev.* **121**, 3892-4044 (2021).

6 Docherty, J. H. *et al.* Transition-Metal-Catalyzed C–H Bond Activation for the Formation of C–C Bonds in Complex Molecules. *Chem. Rev.* **123**, 7692-7760 (2023).

7 Ali, W., Oliver, G. A., Werz, D. B. & Maiti, D. Pd-catalyzed regioselective activation of C(sp2)–H and C(sp3)–H bonds. *Chem. Soc. Rev.* **53**, 9904-9953 (2024).

8 Lovering, F., Bikker, J. & Humblet, C. Escape from Flatland: Increasing Saturation as an Approach to Improving Clinical Success. *J. Med. Chem.* **52**, 6752-6756 (2009).

9 Lovering, F. Escape from Flatland 2: complexity and promiscuity. *MedChemComm* **4**, 515-519 (2013).

10 Roche, S. P. & Porco, J. A. Dearomatization Strategies in the Synthesis of Complex Natural Products. *Angew. Chem. Int. Ed.* **50**, 4068-4093 (2011).

11 Zhuo, C. X., Zhang, W. & You, S. L. Catalytic Asymmetric Dearomatization Reactions. *Angew. Chem. Int. Ed.* **51**, 12662-12686 (2012).

12 Wertjes, W. C., Southgate, E. H. & Sarlah, D. Recent advances in chemical dearomatization of nonactivated arenes. *Chem. Soc. Rev.* **47**, 7996-8017 (2018).

13 Huck, C. J. & Sarlah, D. Shaping Molecular Landscapes: Recent Advances, Opportunities, and Challenges in Dearomatization. *Chem* **6**, 1589-1603 (2020).

14 Ji, P. *et al.* Photochemical dearomative skeletal modifications of heteroaromatics. *Chem. Soc. Rev.* **53**, 6600-6624 (2024).

15 Wiesenfeldt, M. P., Nairoukh, Z., Dalton, T. & Glorius, F. Selective Arene Hydrogenation for Direct Access to Saturated Carbo‐ and Heterocycles. *Angew. Chem. Int. Ed.* **58**, 10460-10476 (2019).

16 Heravi, M., Vazinfard, M. & Faghihi, Z. Recent Applications of Birch Reduction in Total Synthesis of Natural Products. *Curr. Org. Chem.* **19**, 1491–1525 (2015).

17 Wu, W.-T., Zhang, L. & You, S.-L. Catalytic asymmetric dearomatization (CADA) reactions of phenol and aniline derivatives. *Chem. Soc. Rev.* **45**, 1570-1580 (2016).

18 Liebov, B. K. & Harman, W. D. Group 6 Dihapto-Coordinate Dearomatization Agents for Organic Synthesis. *Chem. Rev.* **117**, 13721-13755 (2017).

19 Sarlah, D. & Okumura, M. Arenophile-Mediated Dearomative Functionalization Strategies. *Synlett* **29**, 845-855 (2018).

20 Gaich, T. & Mulzer, J. From Silphinenes to Penifulvins: A Biomimetic Approach to Penifulvins B and C. *Org. Lett.* **12**, 272-275 (2010).

21 Streit, U. & Bochet, C. G. The arene–alkene photocycloaddition. *Beilstein J. Org. Chem.* **7**, 525-542 (2011).

22 Remy, R. & Bochet, C. G. Arene–Alkene Cycloaddition. *Chem. Rev.* **116**, 9816-9849 (2016).

23 Dilmaç, A. M., Spuling, E., de Meijere, A. & Bräse, S. Propellanes—From a Chemical Curiosity to "Explosive" Materials and Natural Products. *Angew. Chem. Int. Ed.* **56**, 5684-5718 (2017).

24 Shi, C.-Y., Zhu, G.-Y., Xu, Y., Teng, M.-Y. & Ye, L.-W. Recent advances in catalytic asymmetric Büchner reaction. *Chin. Chem. Lett.* **34**, 108441 (2023).

25 Buchner, E. & Curtius, T. Ueber die Einwirkung von Diazoessigäther auf aromatische Kohlenwasserstoffe. *Ber. Dtsch. Chem. Ges.* **18**, 2377-2379 (1885).

26 Clayden, J., Knowles, F. E. & Menet, C. J. Stereospecific photochemical ring expansion of lithiated benzamides. *J. Am. Chem. Soc.* **125**, 9278-9279 (2003).

27 Zeng, Q., Dong, K., Huang, J., Qiu, L. & Xu, X. Copper-catalyzed carbene/alkyne metathesis terminated with the Buchner reaction: synthesis of dihydrocyclohepta[b]indoles. *Org. Biomol. Chem.* **17**, 2326-2330 (2019).

28 Mykura, R. *et al.* Synthesis of polysubstituted azepanes by dearomative ring expansion of nitroarenes. *Nat. Chem.* **16**, 771-779 (2024).

29 Patel, S. C. & Burns, N. Z. Conversion of Aryl Azides to Aminopyridines. *J. Am. Chem. Soc.* **144**, 17797-17802 (2022).

30 Mailloux, M. J., Fleming, G. S., Kumta, S. S. & Beeler, A. B. Unified Synthesis of Azepines by Visible-Light-Mediated Dearomative Ring Expansion of Aromatic N-Ylides. *Org. Lett.* **23**, 525-529 (2021).

31 Ito, T. *et al.* Asymmetric Intramolecular Dearomatization of Nonactivated Arenes with Ynamides for Rapid Assembly of Fused Ring System under Silver Catalysis. *J. Am. Chem. Soc.* **143**, 604-611 (2020).

32 Wang, X., Abrahams, Q. M., Zavalij, P. Y. & Doyle, M. P. Highly Regio- and Stereoselective Dirhodium Vinylcarbene Induced Nitrone Cycloaddition with Subsequent Cascade Carbenoid Aromatic Cycloaddition/N-O Cleavage and Rearrangement. *Angew. Chem. Int. Ed.* **51**, 5907-5910 (2012).

33 Xia, J., Liu, J., Yu, Y., Zhang, J. & Huang, X. Divergent Access to Polycyclic N-Heterocyclic Compounds through Büchner-Type Dearomatization Enabled Cycloisomerization of Diynamides under Gold Catalysis. *Org. Lett.* **24**, 4298-4303 (2022).

34 Zhang, L. *et al.* Visible light-driven dearomative ring expansion of (aza)arenes to access dihydrofuran-based polycyclic compounds. *Chem. Sci.* **15**, 8828-8834 (2024).

35 Liu, Z. *et al.* Transition-Metal-Free Intramolecular Carbene Aromatic Substitution/Büchner Reaction: Synthesis of Fluorenes and [6,5,7]Benzo-fused Rings. *Angew. Chem. Int. Ed.* **54**, 3056-3060 (2015).

36 Harada, S., Takenaka, H., Ito, T., Kanda, H. & Nemoto, T. Valence-isomer selective cycloaddition reaction of cycloheptatrienes-norcaradienes. *Nat. Commun.* **15**, 2309 (2024).

37 Li, H. *et al.* Rhodium-Catalyzed Intramolecular Nitrogen Atom Insertion into Arene Rings. *J. Am. Chem. Soc.* **145**, 17570-17576 (2023).

38 Xu, X., Wang, X., Zavalij, P. Y. & Doyle, M. P. Straightforward Access to the [3.2.2]Nonatriene Structural Framework via Intramolecular Cyclopropenation/Buchner Reaction/Cope Rearrangement Cascade. *Org. Lett.* **17**, 790-793 (2015).

39 Strieth-Kalthoff, F., James, M. J., Teders, M., Pitzer, L. & Glorius, F. Energy transfer catalysis mediated by visible light: principles, applications, directions. *Chem. Soc. Rev.* **47**, 7190-7202 (2018).

40 Strieth-Kalthoff, F. & Glorius, F. Triplet Energy Transfer Photocatalysis: Unlocking the Next Level. *Chem* **6**, 1888-1903 (2020).

41 Großkopf, J., Kratz, T., Rigotti, T. & Bach, T. Enantioselective Photochemical Reactions Enabled by Triplet Energy Transfer. *Chem. Rev.* **122**, 1626-1653 (2021).

42 Ju, T. *et al.* Direct Regioselective Reductive Allylation of Imines: Application to Synthesis of Oxazines with Halogenated Reagent. *Org. Lett.* **25**, 8819-8823 (2023).

43 Kwak, D. *et al.* Electroreductive Access to 1,2-Aminoalcohols via Cross Aza-Pinacol Coupling of N-Acyl Diarylketimines and Aldehydes. *Org. Lett.* **26**, 2733-2738 (2023).

44 Ju, T. *et al.* Selective and Catalytic Hydrocarboxylation of Enamides and Imines with CO2 to Generate α,α‐Disubstituted α-Amino Acids. *Angew. Chem. Int. Ed.* **57**, 13897-13901 (2018).

45 Liu, W.-W. *et al.* Photochemical Reductive Carboxylation of N-Benzoyl Imines with Oxalate Accelerated by Formation of EDA Complexes. *ACS Catal.* **14**, 10053-10059 (2024).

46 McNamara, O. A. & Maguire, A. R. The norcaradiene–cycloheptatriene equilibrium. *Tetrahedron* **67**, 9-40 (2011).

47 Janzen, E. G. Spin trapping. *Acc. Chem. Res.* **4**, 31-40 (1971).